

Integrated photonic structures for light trapping in thin-film Si solar cells

Xing Sheng, Steven G. Johnson, Lirong Z. Broderick, Jurgen Michel, and Lionel C. Kimerling

Citation: *Appl. Phys. Lett.* **100**, 111110 (2012); doi: 10.1063/1.3693613

View online: <http://dx.doi.org/10.1063/1.3693613>

View Table of Contents: <http://apl.aip.org/resource/1/APPLAB/v100/i11>

Published by the [American Institute of Physics](#).

Related Articles

Modeling of silicon nanocrystals based down-shifter for enhanced silicon solar cell performance
J. Appl. Phys. **111**, 034303 (2012)

Analytical solution for the photocurrent of solar cells with internal reflection
J. Appl. Phys. **111**, 034502 (2012)

On the design and applicability of nanowire solar cells using low-grade semiconductors
J. Appl. Phys. **111**, 034501 (2012)

Fundamental limits in the external quantum efficiency of single nanowire solar cells
Appl. Phys. Lett. **99**, 263102 (2011)

A semi-analytical model for semiconductor solar cells
J. Appl. Phys. **110**, 123104 (2011)

Additional information on *Appl. Phys. Lett.*

Journal Homepage: <http://apl.aip.org/>

Journal Information: http://apl.aip.org/about/about_the_journal

Top downloads: http://apl.aip.org/features/most_downloaded

Information for Authors: <http://apl.aip.org/authors>

ADVERTISEMENT

NEW!

iPeerReview
AIP's Newest App



**Authors...
Reviewers...
Check the status of
submitted papers remotely!**

AIP | Publishing

Integrated photonic structures for light trapping in thin-film Si solar cells

Xing Sheng,^{1,a)} Steven G. Johnson,² Lirong Z. Broderick,¹ Jurgen Michel,¹
and Lionel C. Kimerling¹

¹Department of Materials Science and Engineering, Massachusetts Institute of Technology, Cambridge, Massachusetts 02139, USA

²Department of Mathematics, Massachusetts Institute of Technology, Cambridge, Massachusetts 02139, USA

(Received 17 January 2012; accepted 23 February 2012; published online 13 March 2012)

We explore the mechanisms for an efficient light trapping structure for thin-film silicon solar cells. The design combines a distributed Bragg reflector (DBR) and periodic gratings. Using photonic band theories and numerical simulations, we discover that light can be scattered into the DBR by gratings, with an unusual way of light trapping different from metal reflectors and photonic crystals. We further investigate the influence of DBR on generated photocurrent in different device configurations. These results would provide new design rules for photonic structures in thin-film solar cells. © 2012 American Institute of Physics. [<http://dx.doi.org/10.1063/1.3693613>]

In this letter, we explain the basic operational principles for an all-dielectric light trapping scheme in solar cells, which integrates periodic gratings and a distributed Bragg reflector (DBR). Light trapping has been studied for a long time for efficiency improvement in thin-film silicon solar cells. Recently, we and others have proposed and experimentally demonstrated the combined DBR and grating structure for effective light trapping.^{1–8} The optical path length in the near infrared spectral range can be significantly enhanced due to the induced light diffraction and reflection. However, the previous reports neither clearly described the mechanisms for such a light trapping design nor analyzed the impacts of the DBR on the solar cell performance, even though the scattering loss in DBRs have been studied in other photonic devices.^{9,10} Here we analyze this structure using fundamental photonic band theory and electromagnetic wave analysis. We discover that the light is scattered into the DBR due to the band folding in the presence of the periodic grating and reflected back at the bottom interface. Therefore, the way of light trapping in this design is different from conventional reflectors based on metals or photonic crystals.^{11–13} Furthermore, we investigate the influence of the bilayers in the DBR on cell performance, showing that the optimal bilayer number should be included for effective reflection and minimized loss.

Our proposed photonic structures for solar cell light trapping are illustrated in Fig. 1, which was first examined in Ref. 1. The DBR consists of alternating amorphous Si (a-Si) and silicon dioxide (SiO₂), working as a one-dimensional (1D) photonic crystal. We assume the refractive indices are 3.6 and 1.45 for a-Si and SiO₂, respectively, and the center wavelength λ_c for reflection is 800 nm. For optimal bandgap size, the thickness of each layer is determined by the quarter-wave criterion ($d = \lambda_c/4n$),¹⁴ so we get $d_{a-Si} = 56$ nm and $d_{SiO_2} = 138$ nm, and the lattice constant $a = d_{a-Si} + d_{SiO_2} = 194$ nm. The photonic band diagrams are calculated using a freely available software package.¹⁵ As shown in the left of Fig. 1, the planar DBR exhibits a complete gap

for both TE and TM polarized light approximately from 650 to 1000 nm, in agreement with previous reports.^{5,8} Therefore, high reflectivity can be obtained in the near-infrared spectral range and utilized for effective light trapping on the back-side of thin-film Si cells.

On top of the DBR, we further implement a one-dimensional grating with a period Λ (see the right of Fig. 1). The grating is assumed to be made of a-Si and SiO₂, with a duty cycle of 0.5 and a thickness of 100 nm. Meanwhile, the period Λ is chosen to be 800 nm for optimal light scattering.¹⁶ Due to the introduced periodicity in the lateral x direction, the photonic bands are folded back into the first Brillouin zone $[-\pi/\Lambda, \pi/\Lambda]$, which completely closes the bandgap. Therefore, the incoming light will be coupled into the propagating modes inside the DBR, regardless of its wavelength and polarization. These results suggest that the combined grating and DBR structures are no longer perfect

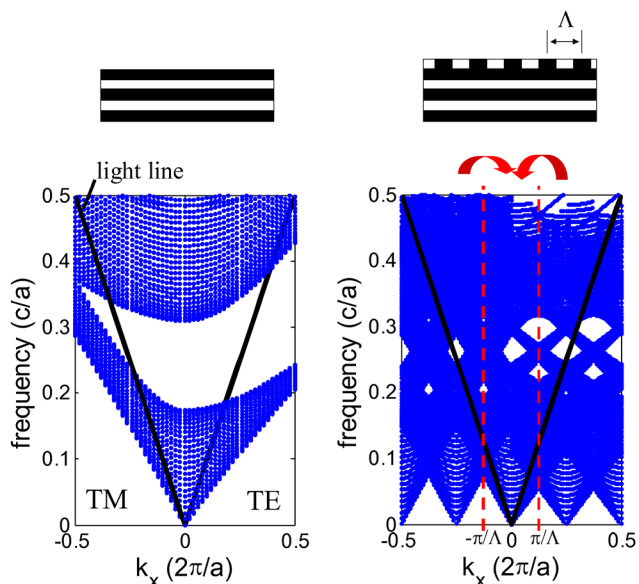


FIG. 1. (Color online) (Left) Band diagram for the DBR made of a-Si/SiO₂ stacks, forming a complete gap with high reflectivity; (right) folded band diagram for the DBR with a period- Λ grating on top, inducing scattering modes inside the DBR. The black solid lines are light lines $\omega = ck_x$.

^{a)}Author to whom correspondence should be addressed. Electronic mail: shengxingstars@gmail.com.

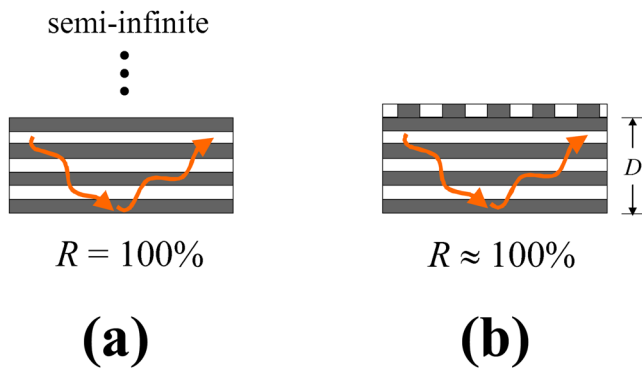


FIG. 2. (Color online) Guided wave propagating in a semi-infinite DBR structure (a) and finite DBR with a grating on top (b).

reflectors, which makes us rethink the light trapping mechanisms of this design.

In Fig. 2 we consider wave propagation in different DBR structures. When a guided wave is incident at the interface between a semi-infinite DBR and air [Fig. 2(a)], it is totally reflected backwards, only evanescently decaying into the air. We can also understand this by the rule of reciprocity, considering that a wave incident from the air will be perfectly reflected if its wavelength falls into the photonic bandgap. If the DBR has a finite thickness D with a grating on top [Fig. 2(b)], the wave can be coupled into the bottom air because of the band folding shown in Fig. 1. However, the photonic local density of state (LDOS) at the interface exponentially decreases as its distance D from the grating increases.¹⁷ When the DBR is thick enough, the coupling into the bottom air becomes negligible. Therefore, the reflection at the finite DBR/air interface can still approach 100%, similar to the case in the semi-infinite DBR [Fig. 2(a)].

To further illustrate wave propagations in thin-film Si devices with different light trapping schemes, we develop device models in Fig. 3. The simulation cell size is $\Lambda = 800$ nm in the lateral x direction, with a periodic boundary condition. The cells are illuminated under normal incidence from air by TE polarized light (with the electric field perpendicular to the incident plane) with a wavelength of 800 nm. The active device layer is $1.5 \mu\text{m}$ crystalline Si(c-Si), with an anti-reflective coating (ARC) made of 70 nm sil-

icon nitride (Si_3N_4). The DBR consists of 5 bilayers of a-Si and SiO_2 . The structural parameters for the DBR and grating are mentioned previously. In addition, an aluminum (Al) reflector is included in Fig. 3(d) for comparison. The optical constants for different materials are found in Ref. 18. The electric field distributions are simulated with the finite-difference time-domain (FDTD) method.¹⁹ The animations for wave propagation can be seen in the enhanced online version of Fig. 3. In the thin-film Si cell without any reflector [Fig. 3(a)], the light is transmitted through the thin-film Si layer into the bottom air, experiencing a single path length. When the planar DBR is placed on the backside of Si [Fig. 3(b)], the electric field evanescently decays into the DBR and is totally reflected backwards, doubling the light path. If the grating layer is embedded between the Si layer and the DBR [Fig. 3(c)], light scattering is induced by the periodicity. Because of the band folding (Fig. 1), the light is also coupled into the DBR. In addition, the scattered light is totally reflected backwards at the planar DBR/air interface in the bottom because of the negligible coupling effect (Fig. 2). The light trapping mechanism for the above design is different from conventional metal (Al) reflectors, in which the light scattering and reflection only occur on the front side of metal because of the skin effect, as seen in Fig. 3(d).

The unusual reflection phenomena described in Fig. 3 suggest that the DBR plays a different role in different device configurations. Results given in Fig. 4 further quantify such effects. Specifically, we evaluate the photon current J_{ph} generated in device structures shown in Fig. 3. The J_{ph} is obtained via the equation $J_{\text{ph}} = e \int A(\lambda)S(\lambda)d\lambda$ in the wavelength range from 750 to 900 nm. The absorption spectra $A(\lambda)$ in the active c-Si layers are obtained by FDTD simulations, while the standard AM1.5G spectrum $S(\lambda)$ is from Ref. 20. Figure 4 plots the influences of the numbers of a-Si/ SiO_2 bilayers in DBR on J_{ph} in the absence and presence of the grating layer, respectively. Here the structures with infinite number of bilayers are simulated by overlapping the DBR stacks with a perfectly matched layer (PML). It should be noted that in the origin point (when the DBR bilayer number is zero) we simply compare two structures with and without grating. In this case, the grating itself can greatly enhance light trapping by scattering effect, even without DBR. For

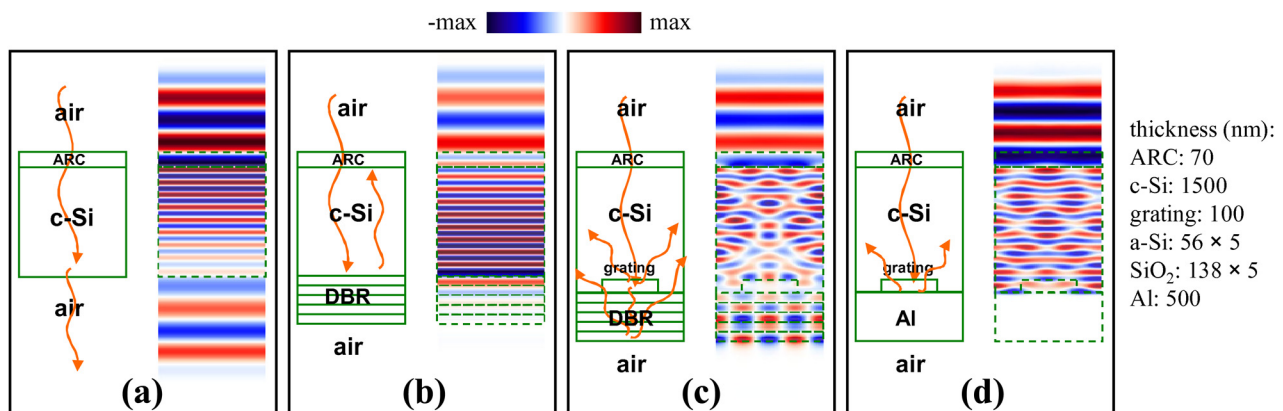


FIG. 3. (Color online) Simulated electric field distribution in planar thin-film c-Si cells with different light trapping schemes: (a) with ARC only; (b) with ARC and DBR; (c) with ARC, grating, and DBR; (d) with ARC, grating, and Al reflector. Thicknesses of different layers are indicated on the right (enhanced online) [URL: <http://dx.doi.org/10.1063/1.3693613.1>].

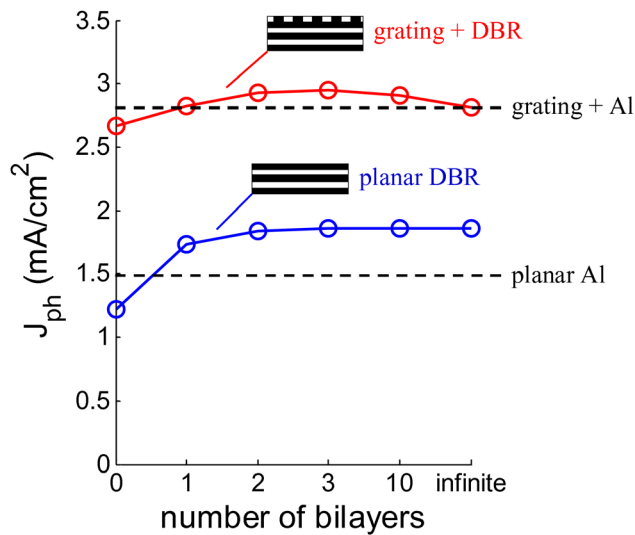


FIG. 4. (Color online) Influence of the number of bilayers in DBR on the integrated J_{ph} (from 750 to 900 nm) for the c-Si solar cells in Fig. 3.

the cell with the planar DBR (blue line), J_{ph} increases with the number of bilayers because of the increased reflectivity. The performance saturates after 3 bilayers are introduced since optical waves evanescently decay into the DBR, as illustrated in Fig. 3(b). In contrast, the cell with both grating and DBR on the backside exhibits a different response (red line). J_{ph} firstly increases with the number of bilayers since certain number of bilayers is needed for sufficient light reflection. However, further increasing the bilayers degrades the cell performance. This is because when we increase the bilayer number, the light experiences a longer path length in the DBR, thus suffering from more parasitic loss due to the absorption in a-Si layers [Fig. 3(c)]. Nevertheless, the combined grating and DBR significantly enhance light path length by scattering. In this spectral range (750–900 nm), the maximum J_{ph} can reach 2.95 mA/cm², in comparison with 1.86 mA/cm² for the device with planar DBR. In addition, the J_{ph} for the cells with the planar Al reflector and combined grating and Al are 1.49 and 2.82 mA/cm², respectively (dashed lines). Both of the results are lower than the corresponding cells with optimal DBR, since Al has higher absorption loss in this spectral range.

To summarize, we understand the mechanisms of a previously reported light trapping design in thin-film solar cells, following the general band theory and electromagnetic analysis. The combined photonic structure with grating and DBR reveals an unusual way of achieving light scattering and reflection, unlike the conventional reflectors based on metals

or photonic crystals with a complete bandgap. As shown in Fig. 4, the trade-off between optical reflection and loss in the DBR (mostly in a-Si layers) should be taken into account when designing the DBR for optimal light trapping. Practically, the materials used for the DBR should have low absorption coefficients to minimize the parasitic loss in the desired spectral range, while maintaining a large refractive index contrast. For example, possible materials having high index and low absorption can be SiC and ZnS.¹⁸ In addition, the bottom surface of the DBR should be planarized to reduce the scattering loss into the bottom medium. We believe these results would also inspire novel designs for various photonic applications.

The authors would like to thank Professors Juejun Hu and Peter Bermel for valuable discussions. This work was supported by the Masdar Institute of Science and Technology.

- ¹L. Zeng, Y. Yi, C. Hong, J. Liu, N. Feng, X. Duan, L. C. Kimerling, and B. A. Alamariu, *Appl. Phys. Lett.* **89**, 111111 (2006).
- ²N. N. Feng, J. Michel, L. Zeng, J. Liu, C. Y. Hong, L. C. Kimerling, and X. Duan, *IEEE Trans. Electron Devices* **54**, 1926 (2007).
- ³P. Bermel, C. Luo, L. Zeng, L. C. Kimerling, and J. D. Joannopoulos, *Opt. Express* **15**, 16986 (2007).
- ⁴J. G. Mutitu, S. Shi, C. Chen, T. Creazzo, A. Barnett, C. Honsberg, and D. W. Prather, *Opt. Express* **16**, 15238 (2008).
- ⁵L. Zeng, P. Bermel, Y. Yi, B. A. Alamariu, K. A. Broderick, J. Liu, C. Hong, X. Duan, J. D. Joannopoulos, and L. C. Kimerling, *Appl. Phys. Lett.* **93**, 221105 (2008).
- ⁶D. Zhou and R. Biswas, *J. Appl. Phys.* **103**, 093102 (2008).
- ⁷X. Sheng, J. Liu, N. Coronel, A. M. Agarwal, J. Michel, and L. C. Kimerling, *IEEE Photon. Tech. Lett.* **22**, 1394 (2010).
- ⁸X. Sheng, J. Liu, I. Kozinsky, A. M. Agarwal, J. Michel, and L. C. Kimerling, *Adv. Mat.* **23**, 843 (2011).
- ⁹Z. Zhang, R. M. von Wurttemberg, J. Berggren, and M. Hammar, *Appl. Phys. Lett.* **91**, 101101 (2007).
- ¹⁰R. K. Price, V. C. Elarde, and J. J. Coleman, *J. Appl. Phys.* **101**, 053116 (2007).
- ¹¹J. M. Gee, in Proceedings of 29th IEEE Photovoltaic Specialists Conference, IEEE, New Orleans, LA, 21-24 May 2002, p. 150.
- ¹²P. G. O'Brien, N. P. Kherani, A. Chutinan, G. A. Ozin, S. John, and S. Zukotynski, *Adv. Mater.* **20**, 1577 (2008).
- ¹³J. Krc, M. Zeman, S. L. Luxembourg, and M. Topic, *Appl. Phys. Lett.* **94**, 153501 (2009).
- ¹⁴L. Rayleigh, *Philos. Mag.* **24**, 145 (1887).
- ¹⁵S. G. Johnson and J. D. Joannopoulos, *Opt. Express* **8**, 173 (2001).
- ¹⁶X. Sheng, S. G. Johnson, J. Michel, and L. C. Kimerling, *Opt. Express* **19**, A841 (2011).
- ¹⁷A. A. Asatryan, K. Busch, R. C. McPhedran, L. C. Botten, C. Martijn de Sterke, and N. A. Nicorovici, *Phys. Rev. E* **63**, 046612 (2001).
- ¹⁸E. Palik, *Handbook of Optical Constants of Solids* (Academic, New York, 1998).
- ¹⁹A. F. Oskooi, D. Roundy, M. Ibanescu, P. Bermel, J. D. Joannopoulos, and S. G. Johnson, *Comput. Phys. Commun.* **181**, 687 (2010).
- ²⁰ASTMG173-03, Standard Tables for Reference Solar Spectral Irradiances: Direct Normal and Hemispherical on 37 degree Tilted Surface (ASTM International, West Conshohocken, Pennsylvania, 2005).